

1    **An MDS-derived cell line and a series of its sublines serve as an *in vitro* model for the**  
2    **leukemic evolution of MDS**

3

4    Running title: A series of cell lines as an MDS progression model

5

6    Jun-ichiro Kida<sup>1</sup>, Takayuki Tsujioka<sup>1</sup>, Shin-ichiro Suemori<sup>1</sup>, Shuichiro Okamoto<sup>1</sup>, Kanae  
7    Sakakibara<sup>1</sup>, Takayuki Takahata<sup>2</sup>, Takahiro Yamauchi<sup>3</sup>, Akira Kitanaka<sup>1</sup>, Yumi Tohyama<sup>4</sup> and  
8    Kaoru Tohyama<sup>1</sup>

9    <sup>1</sup>Department of Laboratory Medicine, Kawasaki Medical School, Okayama, Japan;

10    <sup>2</sup>Central Research Laboratories, Sysmex Corporation, Hyogo, Japan;

11    <sup>3</sup>Department of Hematology and Oncology, Faculty of Medical Sciences, University of Fukui,  
12    Fukui, Japan;

13    <sup>4</sup>Division of Biochemistry, Faculty of Pharmaceutical Sciences, Himeji Dokkyo University,  
14    Hyogo, Japan

15

16    Correspondence to: Kaoru Tohyama, Department of Laboratory Medicine, Kawasaki Medical  
17    School, 577 Matsushima, Kurashiki-City, Okayama 701-0192, Japan

18 E-mail: [ktohyama@med.kawasaki-m.ac.jp](mailto:ktohyama@med.kawasaki-m.ac.jp)

19 phone: 81-86-462-1111 (ext. 25350); fax: 81-86-462-1199

20

21 Conflict of Interest: The authors declare no conflict of interest.

22

23 This work was supported by Grant-in-Aid for Scientific Research from the Japan Society for

24 the Promotion of Science (KAKENHI) and Kawasaki Medical School Project Grant.

25

26 Key words: MDS cell line, whole exome analyses, driver mutation, *histone-H3*(K27M)

27 mutation, leukemic transformation

28

29

30

31

32

33

34



35 Myelodysplastic syndromes (MDS) are clonal hematopoietic stem cell disorders  
36 characterized by ineffective hematopoiesis and increased risk of progression to acute myeloid  
37 leukemia (AML). Occurrence of somatic mutations leads to formation of an abnormal clone  
38 with impaired differentiation, and additional driver mutations lead finally to AML. <sup>1</sup> We  
39 previously established a myelodysplastic cell line MDS92 from the bone marrow of an MDS  
40 patient with deletion of 5q chromosome[del(5q)]. <sup>2,3</sup> MDS92 cells proliferated in the presence  
41 of interleukin(IL)-3 with a tendency for gradual maturation and represented karyotypic  
42 abnormalities including del(5q) (actually der(5)(5;19)), monosomy7 and a point mutation at  
43 codon12 of *NRAS* gene. <sup>2</sup> These characteristics are exclusively compatible with the property  
44 of MDS. Later, a blastic subline MDS-L was established from MDS92. <sup>4</sup> MDS-L cell line  
45 has contributed to the molecular study of MDS with del(5q) <sup>5,6</sup> and therapeutic mechanisms  
46 of lenalidomide. <sup>4,7</sup> MDS-L has also been utilized as an *in vivo* model by transplanting  
47 experiments into immunodeficient mice <sup>8</sup> and for investigation of various drugs expected for  
48 treatment of MDS. <sup>9,10</sup> In addition to MDS-L, we isolated several blastic sublines  
49 independently of one another from the parental MDS92, and further obtained MDS-L-2007  
50 and MDS-LGF from MDS-L in the presence and absence of IL-3, respectively (Figure 1A).  
51 The morphology and surface markers of the cell lines are shown in Supplementary Figure 1

52 and Supplementary Table 1, respectively. In Figure 1A, MDS-Gen implied the mid-stage  
53 cultured cells from bone marrow of the original patient (Pt-BM) for 3 months in the presence  
54 of IL-3 for aiming at establishment of MDS cell lines. We confirmed that the series of cell  
55 lines were all originated from Pt-BM by the short tandem repeat profiling (Supplementary  
56 Table 2).

57 We performed comprehensive, comparative exome analyses on the series of samples by the  
58 next-generation sequencing (NGS) method. Total effective reads per sample ranged from  
59 35,548,000 to 58,711,000 and the average sequencing depth ranged from 46 to 77. Candidate  
60 somatic mutations excluding dbSNP were detected in 406 genes, and 178 mutations were  
61 found in common in all ten samples. Main results are summarized in Supplementary Table 3.

62 As notable mutations, a homozygous, splice donor site mutation of *TP53*(c.672+1G>A;  
63 COSM6906 in COSMIC) was present in all samples including Pt-BM together with  
64 homozygous *TP53*(c.74+14T>C) mutation. MDS-L lost normal TP53 protein probably due to  
65 these mutations (Supplementary Figure 2). *CEBPA*(Q311stop) mutation (heterozygous;  
66 COSM29221) and *NRAS*(G12A) mutation (heterozygous; COSM565) were not detected in  
67 Pt-BM, but they emerged clonally at MDS-Gen stage, and both mutations were inherited by  
68 all subsequent cell lines.

69 Whether *CEBPA*-mutant and *NRAS*-mutant clones were originally latent in Pt-BM or  
70 whether these mutations newly emerged during *in vitro* culture is an important question. To  
71 find the answer, we performed ultra-deep targeted sequencing of *CEBPA* and *NRAS* in Pt-BM,  
72 and the results were as follows: (1) as for *CEBPA*, a single-allele 931C>T(Q311stop) mutation  
73 was detected in 181,059 counts out of 4,044,666 coverages. The detection frequency was  
74 therefore approximately 4.5%, and considering that it was a heterozygous mutation, the  
75 mutant clone must have accounted for approximately 9% of Pt-BM; (2) as for *NRAS*, no  
76 35G>C(G12A) mutation count was detected at all out of 4,712,760 coverages. It implied that  
77 *NRAS*-mutant clone was completely absent from Pt-BM. It was therefore demonstrated that  
78 *CEBPA* mutation was originally present in a part of *TP53*-mutated bone marrow fractions and  
79 this clone was selected during IL-3-containing culture, and it was further suggested that *NRAS*  
80 mutation emerged by chance on the *CEBPA*-mutant clone during *in vitro* culture. Such  
81 accumulated mutations could generate MDS cell lines.

82 Another mutation to which particular attention should be paid is a heterozygous  
83 *histone-H3(HIST1H3C)*(K27M) mutation (*H3*-K27M; COSM1580151) which appeared in  
84 MDS-L, because this mutation would likely be one of the candidates for blastic  
85 transformation. *H3*-K27M mutation is frequently found in pediatric brain stem tumors.<sup>11</sup>

86 *Histone-H3* mutations in hematopoietic tumors are rare, but recently Lehnertz et al. reported  
87 two *H3-K27M* and one *H3-K27I* cases in 615 AML cases.<sup>12</sup> Therefore, there will be a greater  
88 interest in *histone-H3* mutation in myeloid neoplasms. *H3-K27M* mutation was inherited by  
89 MDS-L-2007 which was isolated from MDS-L in the presence of IL-3 but not by MDS-LGF  
90 which was isolated from MDS-L in the absence of IL-3.

91 We found that *H3-K27M* mutation severely affected the whole histone methylation status.  
92 *H3-K27M* protein was expressed in MDS-L and MDS-L-2007, and these cells indicated a  
93 marked reduction in H3-K27 methylation (Figure 1B-C). In contrast, H3-K27 methylation  
94 was conserved in MDS92 and MDS-LGF both of which did not bear *H3-K27M* mutation  
95 (Figure 1B-C). Expression pattern of H3-K27M and H3-K27me2/me3 appeared to be  
96 reciprocal. Immunostaining study showed that MDS-L consisted of both H3-K27  
97 methylation-positive and -negative cells and that MDS-L-2007 was completely lacking in  
98 H3-K27 methylation, whereas MDS-LGF was positive for H3-K27 methylation like as  
99 MDS92 (Figure 1C).

100 To know the difference of *histone-H3* status between MDS-L-2007 and MDS-LGF (both  
101 were originated from MDS-L), we reviewed the sequenced nucleotide reads from NGS and  
102 found that MDS92 and MDS-L had a single nucleotide polymorphism (SNP) at codon32 of

103 one allele of *HIST1H3C*(from ACC to ACG; silent mutation) and that *H3-K27M* mutation  
104 was located in the SNP(ACG)-present allele in MDS-L (Supplementary Figure 3).  
105 Interestingly, in MDS-L-2007 all sequenced reads of the SNP(ACG)-present allele showed  
106 *H3-K27M* mutation, while in MDS-LGF all sequenced reads of the SNP(ACG)-present allele  
107 showed *H3-K27*-wild-type (Supplementary Figure 3). We speculated that MDS-L-2007  
108 inherited *H3-K27M*-mutant allele and expanded in the presence of IL-3, whereas MDS-LGF  
109 inherited *H3-K27*-wild-type allele and survived without IL-3.

110 When MDS-L was cultured in the presence of IL-3, *H3-K27M*-mutant fraction gradually  
111 increased. When MDS-L was cultured without IL-3, *H3-K27M*-mutant fraction gradually  
112 decreased (Figure 1D). This phenomenon was reproducible.

113 To investigate the implication of *H3-K27M* mutation, we tried single-cell cloning from  
114 MDS-L and secured four wild-type clones (MDS-L-K27wt) and seven *H3-K27M*-mutant  
115 clones (MDS-L-K27M). H3 methylation patterns of these clones are shown in Figure 2A. In  
116 all *H3-K27M*-mutant clones, there was a marked reduction in H3-K27me3/2 and a modest  
117 increase in H3-K27ac and H3-K36me3/2. The reason why *H3-K27M* mutation could cause a  
118 drastic decrease in whole methylation status of H3-K27 sites is explained by the fact that  
119 *H3-K27M* protein inhibits histone H3-K27 methyltransferase EZH2 as reported in brain

120 tumor studies.<sup>13</sup> As loss-of-function mutation of *EZH2* often found in myeloid malignancies  
121 is involved in tumorigenesis<sup>14</sup>, *H3-K27M* mutation might have a similar oncogenic  
122 implication as *EZH2* mutation.

123 *H3-K27M*-mutant clones showed rapid growth in the presence of IL-3, but cell  
124 proliferation was suppressed without IL-3 (Supplementary Figure 4). We co-cultured  
125 *H3-K27M*-mutant clones with wild-type clones as a competitive growth experiment in the  
126 presence/absence of IL-3 up to six months. *H3-K27M*-mutant clones became predominant in  
127 the presence of IL-3, whereas wild-type clones were sustained comparatively in the absence  
128 of IL-3 (Figure 2B).

129 Figure 2A also indicated that expression of a tumor-suppressor molecule p16<sup>INK4a</sup> was  
130 reduced in six of the seven *H3-K27M*-mutant clones. Studies on brain tumors reported that  
131 H3-K27 methylation increases exclusively at *p16* locus resulting in reduced p16 expression.<sup>15</sup>  
132 Considering that *H3-K27M*-mutant clones with reduced p16 expression showed more  
133 vigorous proliferation than wild-type clones, p16 might be a therapeutic target. Treatment  
134 with an *EZH2* inhibitor EPZ-6438 caused growth suppression of *H3-K27M*-mutant clones as  
135 well as wild-type clones with demethylation of H3-K27 site particularly of wild-type clones,  
136 and more importantly, involved obvious recovery of p16 expression in *H3-K27M*-mutant

clones (Supplementary Figure 5 and Figure 2C).

Although a histone-demethylase JMJD3 inhibitor GSK-J4 was reported to inhibit *H3-K27M*-mutated pediatric brain stem tumors,<sup>11</sup> GSK-J4 exerted only non-specific growth inhibitory effect on both *H3-K27M*-mutant and wild-type clones (data not shown), and it is unclear whether the treatment for *H3-K27M*-mutated brain tumors can be applied to hematological malignancies.

As already noted, we obtained interesting data on the relation of *H3-K27M* mutation to IL-3-dependency. When MDS-L was cultured in the presence of IL-3, *H3-K27M*-mutant clones proliferated dominantly (Figures 1D and 2B) and MDS-L-2007 subline was one outcome. Conversely, when MDS-L was maintained without IL-3, the majority of cells died and most of surviving fractions were wild-type clones (Figures 1D and 2B), and in this way MDS-LGF subline was established. This aggressive but strictly IL-3-dependent growth of *H3-K27M*-mutant clones implies a relation of *H3-K27M* mutation with enhanced growth signal via IL-3. The phenomenon that the dominant fraction was replaced according to the presence or absence of IL-3 suggests that growth advantage of mutant clones is affected by environmental factors such as growth factors. These data raise a possibility that even if neoplastic clones emerge, their expansion might be influenced not only by genetic/epigenetic

status but also by surrounding environmental factors.

In this study, we established a myelodysplastic cell line and subsequent blastic sublines. We confirmed that accumulated gene mutations were involved in the establishment of MDS cell lines and progression to AML phenotypes (Figure 2D). This series of cell lines will be a useful tool as an *in vitro* model for leukemic evolution of MDS.

## **Acknowledgements**

The authors thank Dr. Takanori Ueda (Fukui Medical University, Fukui, Japan) for his outstanding supervision and contribution to ethical approval, Drs. Hiroya Kirimura and Kengo Gotoh (Central Research Laboratories, Sysmex Corporation, Hyogo, Japan) for genetic analysis. The authors also thank Ms. Aki Kuyama for editorial assistance. This work was supported by Grant-in-Aid for Scientific Research from the Japan Society for the Promotion of Science (KAKENHI) and Kawasaki Medical School Project Grant.

## **Conflict of Interest**

The authors declare no conflict of interest.



171

172

173   Supplementary information is available at Leukemia's website

174

175   **References**

176   1.       Cazzola M, Della Porta MG, Malcovati L. The genetic basis of myelodysplasia and  
177   its clinical relevance. *Blood*. 2013;122(25):4021-34.

178   2.       Tohyama K, Tsutani H, Ueda T, Nakamura T, Yoshida Y. Establishment and  
179   characterization of a novel myeloid cell line from the bone marrow of a patient with the  
180   myelodysplastic syndrome. *Br J Haematol*. 1994;87:235-42.

181   3.       Drexler HG, Dirks WG, Macleod RA. Many are called MDS cell lines: one is  
182   chosen. *Leukemia research*. 2009;33(8):1011-6.

183   4.       Matsuoka A, Tochigi A, Kishimoto M, Nakahara T, Kondo T, Tsujioka T, et al.  
184   Lenalidomide induces cell death in an MDS-derived cell line with deletion of chromosome 5q  
185   by inhibition of cytokinesis. *Leukemia*. 2010;24(4):748-55.

186   5.       Li L, Sheng Y, Li W, Hu C, Mittal N, Tohyama K, et al. beta-Catenin Is a Candidate  
187   Therapeutic Target for Myeloid Neoplasms with del(5q). *Cancer research*.

188 2017;77(15):4116-26.

189 6. Fang J, Liu X, Bolanos L, Barker B, Rigolino C, Cortelezzi A, et al. A calcium- and  
190 calpain-dependent pathway determines the response to lenalidomide in myelodysplastic  
191 syndromes. *Nature medicine*. 2016;22(7):727-34.

192 7. Kronke J, Fink EC, Hollenbach PW, MacBeth KJ, Hurst SN, Udeshi ND, et al.  
193 Lenalidomide induces ubiquitination and degradation of CK1alpha in del(5q) MDS. *Nature*.  
194 2015;523(7559):183-8.

195 8. Rhyasen GW, Bolanos L, Fang J, Jerez A, Wunderlich M, Rigolino C, et al.  
196 Targeting IRAK1 as a therapeutic approach for myelodysplastic syndrome. *Cancer cell*.  
197 2013;24(1):90-104.

198 9. Hyoda T, Tsujioka T, Nakahara T, Suemori S, Okamoto S, Kataoka M, et al.  
199 Rigosertib induces cell death of a myelodysplastic syndrome-derived cell line by DNA  
200 damage-induced G2/M arrest. *Cancer Sci*. 2015;106(3):287-93.

201 10. Tsujioka T, Yokoi A, Itano Y, Takahashi K, Ouchida M, Okamoto S, et al.  
202 Five-aza-2'-deoxycytidine-induced hypomethylation of cholesterol 25-hydroxylase gene is  
203 responsible for cell death of myelodysplasia/leukemia cells. *Scientific reports*. 2015;5:16709.

204 11. Hashizume R, Andor N, Ihara Y, Lerner R, Gan H, Chen X, et al. Pharmacologic

inhibition of histone demethylation as a therapy for pediatric brainstem glioma. *Nature medicine*. 2014;20(12):1394-6.

12. Lehnertz B, Zhang YW, Boivin I, Mayotte N, Tomellini E, Chagraoui J, et al. H3(K27M/I) mutations promote context-dependent transformation in acute myeloid leukemia with RUNX1 alterations. *Blood*. 2017;130(20):2204-14.

13. Lewis PW, Muller MM, Koletsky MS, Cordero F, Lin S, Banaszynski LA, et al. Inhibition of PRC2 activity by a gain-of-function H3 mutation found in pediatric glioblastoma. *Science (New York, NY)*. 2013;340(6134):857-61.

14. Iwama A. Polycomb repressive complexes in hematological malignancies. *Blood*. 2017;130(1):23-9.

15. Mohammad F, Weissmann S, Leblanc B, Pandey DP, Hojfeldt JW, Comet I, et al. EZH2 is a potential therapeutic target for H3K27M-mutant pediatric gliomas. *Nature medicine*. 2017;23(4):483-92.

## Figure Legends

**Figure 1. The overview of the series of MDS cell lines and histone H3-K27 methylation**

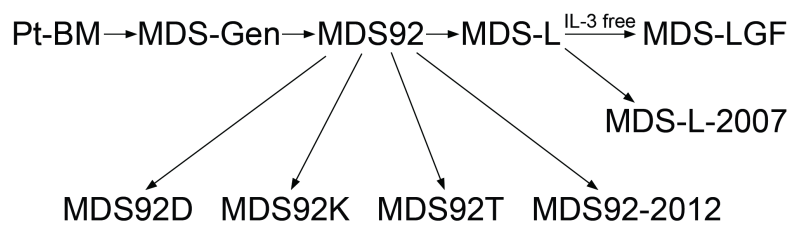
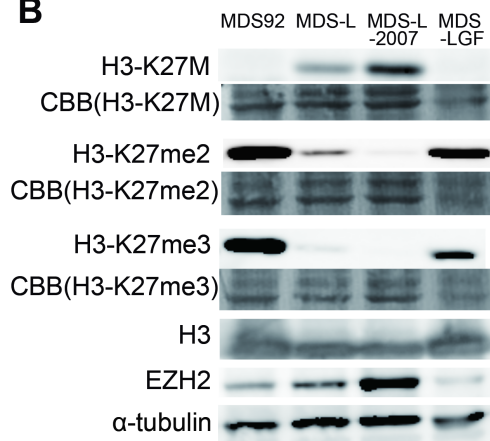
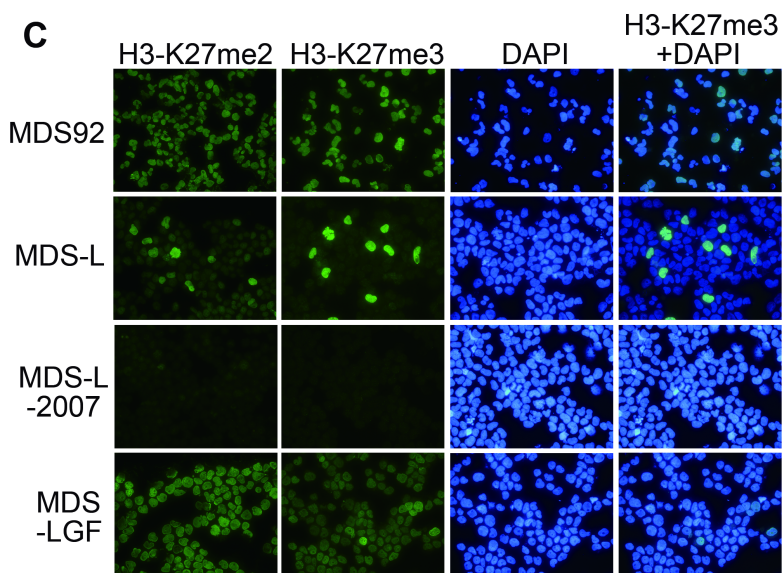
**status.**

(A) The overview of the establishment of MDS92 and the evolution of the sublines. (B) Histone H3-K27 methylation status of the cell lines by immunoblotting analysis. Protein expression of EZH2 is also indicated. CBB stain and  $\alpha$ -tubulin were shown as a loading control. (C) Histone H3-K27 methylation status by immunofluorescence analysis. Original magnification was  $\times 600$ . (D) Presence or absence of IL-3 in culture alters the proportion of *H3-K27M*-mutant fraction. MDS-L cells were cultured in the presence or absence of IL-3 for five months, and the cells were immunostained by anti-H3-K27me3 antibody. Original magnification was  $\times 200$ .

**Figure 2. Impact of *H3-K27M* mutation on IL-3-dependent growth and a schematic model of the series of MDS cell lines and the progression to AML phenotypes.**

(A) H3 methylation patterns between *H3-K27*-wild-type clones and *H3-K27M*-mutant clones from MDS-L. In *H3-K27*-wild-type clones (clone1 to 4) and *H3-K27M*-mutant clones (clone1 to 7), comprehensive methylation/acetylation status of histone H3 was examined by immunoblotting analysis. CBB stain and  $\alpha$ -tubulin were shown as a loading control. (B) Competitive growth experiment by co-culture of *H3-K27*-wild-type and *H3-K27M*-mutant

239 clones in the presence or absence of IL-3. We mixed the same number of eight cloned cells  
240 (wt1 to wt4, and K27M1 to K27M4) and started co-culture in the presence or absence of IL-3.  
241 The cells were immunostained by anti-H3-K27me3 antibody. Original magnification was  
242 ×200. (C) Effects of an EZH2 inhibitor EPZ-6438 on H3-K27 methylation status and  
243 expression of p16 in wild-type and mutant clones. *H3-K27*-wild-type clones (wt1 and wt2)  
244 and *H3-K27M*-mutant clones (K27M1 to K27M4) were treated with EPZ-6438 for 14 d, and  
245 the amount of H3-K27me2, H3-K27me3 and p16 was examined by immunoblotting analysis.  
246 (D) A schematic model indicating the accumulation of gene mutations involved in the  
247 establishment of the series of MDS cell lines and the progression to AML phenotypes. A  
248 homozygous *TP53* mutation was originally present in whole Pt-BM, and *CEBPA* mutation  
249 was also originally present in a small fraction of Pt-BM. *CEBPA*-mutant clone began to  
250 proliferate and *NRAS* mutation emerged by chance during the IL-3-containing culture leading  
251 to MDS92 cell line. MDS92 contained multiple blastic clones and some of them were isolated  
252 independently as blastic sublines. *Histone-H3-K27M* mutation was newly detected in MDS-L.  
253 MDS-L cells were a mixture of *H3-K27M*-mutant and wild-type clones. Long-term culture of  
254 MDS-L in the presence and absence of IL-3 generated MDS-L-2007 (*H3-K27M*-mutant) and  
255 MDS-LGF (*H3-K27*-wild-type), respectively.

**A****B****C****D**